Cross-relaxation dynamics of optically excited N-V centers in diamond

Eric van Oort and Max Glasbeek
Laboratory for Physical Chemistry, University of Amsterdam, Nieuwe Achtergracht 127, 1018 WS Amsterdam, The Netherlands
(Received 5 April 1989)

Upon the cw optical excitation of N-V centers in diamond, a spin alignment in the ensemble of nonexcited N-V defects in the electron spin-triplet ground state is induced. When the diamond sample is subjected to magnetic fields of suitable directions and strengths, cross relaxation (CR) and level anticrossing are found to affect the ground-state spin alignment as well as the intensity of the emission due to the photoexcited N-V centers. In this paper, a study of the dynamics involved in the cross-relaxation and autocrossing processes is reported, utilizing techniques for the optical detection of spin-coherent transients. A major finding is that when CR conditions prevail, the stimulated spin-echo and spin-locking signals decay at a rate about three times faster than in the situation in which CR does not occur. The results are accounted for by considering the magnetic dipole-dipole interactions within the ensemble of N-V centers in the triplet ground state in a memory function approach.

I. INTRODUCTION

The N-V center in type-Ib diamond consists of a substitutional nitrogen atom adjacent to a carbon atom vacancy containing one electron.[1] The center gives rise to a zero-phonon line, peaked at 638 nm, with a phonon sideband to higher and lower energy in low-temperature absorption and emission, respectively. Whereas previous EPR results seemed indicative of a spin-singlet ground state and a metastable triplet excited state for the N-V center defect,[2,3] recent two-laser hole-burning results gave evidence for a triplet-spin ground state (^3A).[4] Optically detected spin coherence[5] and optical hole-bleaching experiments in the presence of a magnetic field[6] further substantiated that the N-V center has an electronic triplet ground state.

In this paper, we report on cross-relaxation (CR) and level-anticrossing (LAC) effects observed in the optical emission of the N-V center when the magnitude of an externally applied magnetic field is swept. It is discussed that upon optical pumping the N-V center a spin alignment in the triplet ground state is produced and that this spin alignment is relaxed when for certain magnetic field strengths the N-V centers become resonant with defects of a different spin temperature.

The dynamics of the CR process is examined by means of time-resolved spin-coherent transient measurements of the N-V center in its triplet ground state. In the experiments use is made of techniques for the optical detection of spin coherence.[7] The techniques are well known in studies of excited state dynamics. Here we show that the method is also applicable in the case that the molecular defect has a triplet ground state and a luminescent excited state. The idea is simply that the laser-induced spin alignment in the ensemble of N-V centers in the triplet ground state is, upon the application of a microwave $\pi/2$ pulse resonant with the zero-field triplet-spin transition of the N-V center ($D=2.88$ GHz), partly converted into spin coherence. Time-dependent interactions give rise to a loss of the phase coherence. After the elapse of time, the residual coherence is converted back into a spin alignment by means of a final microwave $\pi/2$ pulse (the probe pulse). In general, the initial and final spin alignments will thus be different. In turn, the generated change in the ground-state spin alignment will effect a slight change in the population of the fluorescent excited state when the N-V defect system is continuously optically pumped by the laser. The ensuing change in the fluorescence intensity of the N-V center thus is representative of the temporal behavior of the spin coherence of the N-V center system.

In this work, the coherence experiments include the measurement of stimulated spin-echo decays (SED) and spin-locking decays (SLD) for the N-V center system in magnetic fields along [111] and [001] crystallographic directions. A main result is the enhancement of the SED and SLD rate constants by a factor of about 3 when magnetically inequivalent N-V centers become resonant. The spin dynamics results are, as in related work,[8,9] discussed using a memory-function approach.[10] In Sec. II, it is reviewed which terms in the magnetic dipole-dipole interaction between the spin-coherent N-V centers and the resonantly coupled (nonexcited) N-V centers contribute to the relaxation of the spin coherence. We find that the experimental results (cf. Sec. IV) can be satisfactorily explained by an explicit consideration of the "dynamic" secular terms of the dipole-dipole interaction among resonant N-V centers (Sec. V).

II. MEMORY-FUNCTION APPROACH FOR CR DYNAMICS

In considering the decay with time of the probed spin coherence components, S_3 and S_1 in the SED and SLD experiments, respectively, we make use of a Zwanzig-Mori projection-operator formalism.[10] In this formalism, the time development of the spin magnetization S_i is governed by an equation of motion of the form[8,11]

$$\frac{\partial\langle S_i(t)\rangle}{\partial t} = -\int_0^t dt' K_i(t,t')\langle S_i(t')\rangle \ . \tag{1}$$

The memory function $K_i(t,t')$ develops in our system from magnetic dipolar couplings between the *probed N-V* center triplet spins (henceforth called A spins) and randomly *fluctuating* distant *N-V* center triplet spins (called B spins). The observables S_3 and S_1 are in the α-, β-, γ-matrix notation defined as

$$\langle S_3\rangle = \mathrm{Tr}(\rho S_3) = \rho_{\beta\beta} - \rho_{\gamma\gamma} \tag{2a}$$

and

$$\langle S_1\rangle = \mathrm{Tr}(\rho S_1) = \rho_{\beta\gamma} - \rho_{\gamma\beta} \ , \tag{2b}$$

where the A-spin levels α, β, and γ are as in Fig. 1(a).

Previously, expressions for the memory function have been derived for the case of magnetic dipolar couplings between defects in a photoexcited triplet state and defects in an electron spin-doublet ground state.[8,12] Analogously, we consider now the memory functions for the observables $\langle S_3(t)\rangle$ and $\langle S_1(t)\rangle$, arising from dipolar interactions between A and B triplet spins.

We have

$$K_i(t,t') = \frac{\mathrm{Tr}\{[S_i,H(t)]\exp(-iH_B t_c)[H(t'),S_i]\exp(iH_B t_c)\}}{\mathrm{Tr}(S_i S_i)} \ , \tag{3}$$

where

$$t_c = t - t' \ , \tag{4}$$

$$H(t) = H_{AB}(t) + H_B \ , \tag{5}$$

$$H_{AB}(t) = \sum_{A,B} h_{AB}(t) \ , \tag{6}$$

and

$$h_{AB} = d_{xB}S_{xA}(t) + d_{yB}S_{yA}(t) + d_{zB}S_{zA}(t) \tag{7}$$

with

$$d_{xB} = [(1-3X_{AB}^2)S_{xB} - 3X_{AB}Y_{AB}S_{yB} - 3Z_{AB}X_{AB}S_{zB}] \times (g_A g_B \mu_B / r_{AB}^3) \tag{8}$$

and analogous expressions for d_{yB} and d_{zB}. X_{AB}, Y_{AB}, and Z_{AB} denote the direction cosines of the AB axis with respect to the A-spin triplet fine-structure axes. H_A and H_B represent the total spin Hamiltonians for the ensembles of A and B spins, respectively. For axially symmetric triplet A and B spins, the memory functions of interest here become

$$K_3(t,t') \sim \sum_{A,B} \{[\langle d_{xB}d_{xB}(t_c)\rangle + \langle d_{yB}d_{yB}(t_c)\rangle](\cos\omega_{\alpha\gamma}t_c + 4\cos\omega_{\beta\gamma}t_c) + [\langle d_{yB}d_{xB}(t_c)\rangle - \langle d_{xB}d_{yB}(t_c)\rangle](\sin\omega_{\alpha\gamma}t_c - 4\sin\omega_{\beta\gamma}t_c)\} \tag{9}$$

and

$$K_1(t,t') \sim \sum_{A,B} \{[\langle d_{xB}d_{xB}(t_c)\rangle + \langle d_{yB}d_{yB}(t_c)\rangle](\cos\omega_{\alpha\gamma}t_c + 2\cos\omega_{\beta\gamma}t_c) + 2\langle d_{zB}d_{zB}(t_c)\rangle + [\langle d_{yB}d_{xB}(t_c)\rangle - \langle d_{xB}d_{yB}(t_c)\rangle](\sin\omega_{\alpha\gamma}t_c - 2\sin\omega_{\beta\gamma}t_c)\} \ , \tag{10}$$

where $\omega_{\alpha\gamma}$ and $\omega_{\beta\gamma}$ refer to the A-spin resonance frequencies [cf. Fig. 1(a)], and

$$\langle d_{xB}d_{xB}(t_c)\rangle = \mathrm{Tr}[d_{xB}\exp(-iH_B t_c)d_{xB}\exp(iH_B t_c)] \tag{11}$$

with analogous expressions for the other B-spin time correlation functions.

The B-spin auto- and cross-correlation functions involving d_{xB} and d_{yB} oscillate at the B-spin resonance frequencies. In the general case that A and B spins are nonresonant (i.e., A and B spins belong to magnetically inequivalent sites for the system in a magnetic field), multiplication of the B-spin correlation functions with the A-spin oscillatory factors in Eqs. (9) and (10) yields products that are still oscillatory at frequencies corresponding to the sum and differences of A and B spin frequencies. After summation over all A,B pairs in Eqs. (9) and (10) their contribution to the memory function then rapidly dies out. In the event, however, that the A and B spins are resonant, the time correlation functions of the B spins contain Fourier components at a frequency of $\omega_{\alpha\gamma}$ and/or $\omega_{\beta\gamma}$. Ensemble averaging then yields "dynamic" secular terms to $K_i(t,t')$ and an enhanced relaxation rate corresponding to cross-relaxation emerges.

To further evaluate the contribution of the various terms in Eqs. (9) and (10), it is remarked that the ensemble of B spins (which cause the A-spin relaxation) consists

of N-V center defects with main axes along the same directions as the A spins, and of B spins for which the spin axes are oriented along different directions. When a magnetic field along the [111] direction is applied, the former subensemble (henceforth labeled as subensemble I) will form the ensemble of magnetically equivalent defects, whereas the latter subensemble (labeled II) will be comprised of all other defects (the magnetically inequivalent B-spin defects characterized by z^{II} axes at an angle of $\theta=109°28'$ turned away from the A-spin z^{I} axis). The relative orientation of the fine-structure main axes of members of subensembles I and II is given schematically in Fig. 1(b). The N-V centers possess axial local symmetry and hence the y^{I} axis of the fine-structure tensor can be picked arbitrarily in a plane perpendicular to z^{I}; the same applies for y^{II} with respect to z^{II}. We choose y^{I} and y^{II} to coincide so that $y^{\mathrm{I,II}}=0$. The memory functions may now be written as

$$K_i(t,t')=K_i^{\mathrm{I}}+K_i^{\mathrm{I,II}} . \tag{12}$$

In Eq. (12), K_i^{I} has a form as in Eq. (9) or Eq. (10) with the limitation that the summation is restricted to magnetically equivalent A and B spins belonging to subensemble I only; likewise, $K_i^{\mathrm{I,II}}$ is of the form of Eq. (9) or Eq. (10), but now the summation involves A spins of subensemble I and fluctuating B spins belonging to subensemble II. Note that when $\mathbf{H}\|[111]$, the number of spins in subensemble II is three times the number of spins in subensemble I.

When the magnetic field is such that otherwise magnetically inequivalent A and B spins become accidentally degenerate in energy, cross relaxation is expected to enhance the spin dynamics. Evidently, with reference to Eq. (12) and the aforementioned discussion, we anticipate that the dynamics enhancement is characterized by the $K_i^{\mathrm{I,II}}$ term in Eq. (12) which, when the A and B spins are resonant, is no longer averaged out. To calculate the relative change of $K_i(t,t')$ due to CR, we have to consider the correlation functions as they appear in K_i^{I} and $K_i^{\mathrm{I,II}}$.

To this end, we first consider $K_i^{\mathrm{I,II}}$. The B-spin correlation function $\langle d_{xB}d_{xB}(t_c)\rangle$ takes the form

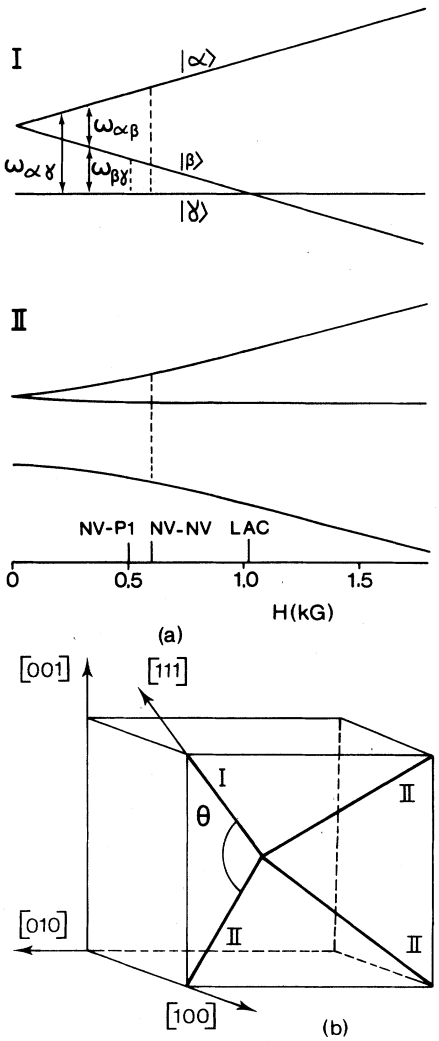

FIG. 1. (a) Magnetic field dependence of triplet sublevel energies for the magnetic field oriented along a [111] crystal axis in the N-V center subensembles I and II. $\omega_{\alpha\beta}$, $\omega_{\alpha\gamma}$, and $\omega_{\beta\gamma}$ denote resonance frequencies for subensemble I. Magnetic field strengths relevant for NV-$P1$ and NV-NV cross relaxation, and level anticrossing, are as indicated. (b) Relative orientation of N-V center main axes in subensembles I and II. $\theta=109°28'$.

$$\langle d_{xB}d_{xB}(t_c)\rangle=[(1-3X_{AB}^2)^2\langle S_{xB}S_{xB}(t_c)\rangle+9(X_{AB}Z_{AB})^2\langle S_{zB}S_{zB}(t_c)\rangle$$
$$-3(1-3X_{AB}^2)X_{AB}Z_{AB}\langle S_{zB}S_{xB}(t_c)\rangle-3(1-3X_{AB}^2)X_{AB}Z_{AB}\langle S_{xB}S_{zB}(t_c)\rangle] . \tag{13}$$

The contribution of Eq. (13) to $K_i^{\mathrm{I,II}}$ involves B spins of subensemble II, thus transformation of $\langle S_{xB}S_{xB}(t_c)\rangle$ in Eq. (13) into the B-spin main axis frame xB^{II}, yB^{II}, zB^{II} yields

$$\langle S_{xB}S_{xB}(t_c)\rangle=\langle S_{zB}^{\mathrm{II}}S_{zB}^{\mathrm{II}}(t_c)\rangle\sin^2\theta+\langle S_{xB}^{\mathrm{II}}S_{xB}^{\mathrm{II}}(t_c)\rangle\cos^2\theta-\langle S_{zB}^{\mathrm{II}}S_{zB}^{\mathrm{II}}(t_c)\rangle\sin\theta\cos\theta-\langle S_{xB}^{\mathrm{II}}S_{xB}^{\mathrm{II}}(t_c)\rangle\sin\theta\cos\theta , \tag{14}$$

where θ, the angle between the z^{I} axis of the A spin of subensemble I and the z^{II} axis of the B spin of subensemble II, equals 109°28′, and

$$S_{zB}^{\mathrm{II}}(t_c)=\exp(-iH_Bt_c)S_{zB}^{\mathrm{II}}\exp(iH_Bt_c) , \tag{15}$$

H_B being, as before, the full spin Hamiltonian for the triplet B spin. Similarly, the other correlation functions of Eq. (13) may be rewritten in terms of the B-spin operators of the main axes system of the B-spin site. Substitution of Eq. (14) and the other rewritten correlation functions in Eq. (13) results in a transformed form of $\langle d_{xB}d_{xB}(t_c)\rangle$ which contains no other correlation func-

TABLE I. Expressions for the B-spin factor appearing in K_i^{I} and $K_i^{\mathrm{I,II}}$.

Memory-function component	Typical form of terms to be summed in Eqs. (9) and (10)[a]	Average value of memory-function component $(\bar{K}_i)$[b]
K_3^{I}	$5[(1-3X_{AB}^2)^2+1]$	72π
$K_3^{\mathrm{I,II}}$	$5[\frac{1}{3}(1-3X_{AB}^2)^2+8X_{AB}^2Z_{AB}^2-\frac{4}{3}\sqrt{2}(1-3X_{AB}^2)X_{AB}Z_{AB}+1]$	$(584/9)\pi$
K_1^{I}	$3[(1-3X_{AB}^2)^2+2(1-3Z_{AB}^2)^2]$	56π
$K_1^{\mathrm{I,II}}$	$3[\frac{1}{9}(1-3X_{AB}^2)^2+8X_{AB}^2Z_{AB}^2-\frac{4}{3}\sqrt{2}(1-3X_{AB}^2)X_{AB}Z_{AB}+1]$ $+2[\frac{1}{9}(1-3Z_{AB}^2)^2+8X_{AB}^2Z_{AB}^2-\frac{4}{3}\sqrt{2}(1-3Z_{AB}^2)X_{AB}Z_{AB}]$	$(440/9)\pi$
	$r_3=(\bar{K}_3^{\mathrm{I}}+3\bar{K}_3^{\mathrm{I,II}})/\bar{K}_3^{\mathrm{I}}\cong 3.7$	
	$r_1=(\bar{K}_1^{\mathrm{I}}+3\bar{K}_1^{\mathrm{I,II}})/\bar{K}_1^{\mathrm{I}}\cong 3.6$	

[a]This column was obtained assuming $\langle S_{zB}S_{zB}(t_c)\rangle\cong\langle S_{xB}S_{xB}(t_c)\rangle\cos\omega t_c\cong\langle S_{yB}S_{yB}(t_c)\rangle\cos\omega t_c$, and deleting the factor $k=\langle S_{zB}S_{zB}(t_c)\rangle$ common to all terms in Eq. (9) or Eq. (10).
[b]Average value $(\bar{K}_i)$ was obtained as $K_i=\int K_i\sin\theta\,d\theta\,d\phi$, where K_i takes the forms as given in the second column.

tions (in the B-spin main frame) than those already mentioned in Eq. (14). Eventually, the function $\langle d_{xB}d_{xB}(t_c)\rangle$ when substituted in $K_i^{\mathrm{I,II}}$ has to be multiplied with oscillatory factors containing A-spin frequencies and the summation over all A and B spins has to be performed. Thus all correlation functions appearing in $\langle d_{xB}d_{xB}(t_c)\rangle$ which cannot possibly oscillate at the A-spin frequencies (whatever the magnitude of the applied magnetic field) may be left out. In particular this implies that terms containing $\langle S_{zB}^{\mathrm{II}}S_{zB}^{\mathrm{II}}(t_c)\rangle$, $\langle S_{xB}^{\mathrm{II}}S_{zB}^{\mathrm{II}}(t_c)\rangle$, or $\langle S_{zB}^{\mathrm{II}}S_{xB}^{\mathrm{II}}(t_c)\rangle$ may be ignored. Furthermore, since $Y_{AB}=0$, one has $S_{yB}^{\mathrm{I}}=S_{yB}^{\mathrm{II}}$, and

$$\langle d_{yB}d_{yB}(t_c)\rangle=\langle S_{yB}^{\mathrm{II}}S_{yB}^{\mathrm{II}}(t_c)\rangle=\langle S_{xB}^{\mathrm{II}}S_{xB}^{\mathrm{II}}(t_c)\rangle\ . \tag{16}$$

The resulting expression for the B-spin factor appearing in $K_i^{\mathrm{I,II}}$ is collected in Table I. The procedure for obtaining the contribution of the magnetic interaction between magnetically equivalent A and B spins to the memory function K_i^{I} is analogous. The expressions obtained for the B-spin factors K_i^{I} are included in Table I.

To estimate the relative change of K_i in going from a CR situation (as in zero field) to a non-CR situation (i.e., when H is nonzero), the geometrical factors in the expressions in Table I have been averaged by integration of the direction cosine functions over all possible values of the orientation of $\mathbf{R}_{AB}$. The averaged results for the various K_i^{I} and $K_i^{\mathrm{I,II}}$ components under CR and non-CR conditions are included in Table I also. The memory function in the presence of CR is proportional to $\bar{K}_i^{\mathrm{I}}+3\bar{K}_i^{\mathrm{I,II}}$ since for the N-V center the number of magnetically inequivalent B spins belonging to subensemble II is three times the number of magnetically equivalent B spins of ensemble I. It is thus found that the ratio of the memory functions in the presence and absence of CR, respectively, is given as $r_i=(\bar{K}_i^{\mathrm{I}}+3\bar{K}_i^{\mathrm{I,II}})/\bar{K}_i^{\mathrm{I}}$. We conclude that the estimated CR enhancement factor in the stimulated-echo decay experiment is $r_3=3.7$. Similarly, it is estimated that the CR enhancement factor for the spin-locking decay rate constant is $r_1=3.6$.

III. EXPERIMENT

The diamond crystal was the same as previously.[5] The crystal was mounted inside a slow-wave helix immersed in a pumped liquid-helium bath ($T=1.4$ K). Optical excitation was at 514 nm using a cw Ar^+-ion laser with 200 mW output power. The fluorescence emitted perpendicular to the exciting light was focused on the entrance slit of a Monospek 1000 grating monochromator. Photodetection was at 638 nm using a GaAs photomultiplier tube. The optically detected magnetic resonance (ODMR) and spin-echo spectrometer used for the optical detection of spin-coherent transients has been described previously.[8] Microwave pulse trains at a microwave frequency in the range between 1 and 6 GHz were applied at a repetition rate of 30 Hz. The microwave-induced changes in the emission near 638 nm were monitored using phase-sensitive detection techniques. Magnetic fields were applied by means of superconducting Helmholtz coils, immersed in the helium bath, fed by a regulated power supply.

IV. RESULTS

A. CR and LAC effects in N-V center emission

Figure 2 presents the derivative of the magnetic field-induced changes in the intensity of the N-V center emission when the magnitude of a magnetic field along a [111] direction of the crystal is increased. The signal was obtained using amplitude modulation of the external field (at a repetition rate of 30 Hz) and applying phase-sensitive detection of the N-V center fluorescence. Sudden changes in the emission intensity are observed when the magnetic field values become $H=514$ G, $H=600$ G, and $H=1030$ G, respectively. In Fig. 2(d) the signal peaking near 514 G is presented on an enlarged scale. In addition to the main peak at 514 G, hyperfine lines shifted by ± 15 G, ± 19 G from the central main peak are found.

Recently, for exactly the same field strengths, sudden changes were observed in the intensity of the no-phonon optical-absorption line when performing optical hole-

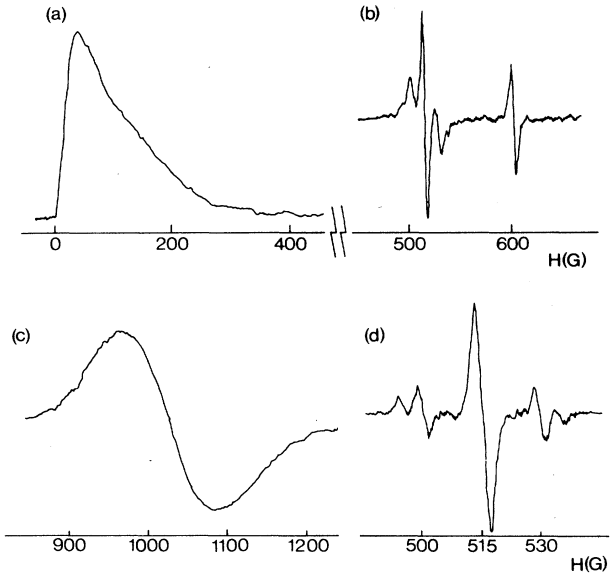

FIG. 2. Derivative of the intensity changes in the zero-phonon emission of the N-V center as induced by a magnetic field. $\mathbf{H}\|[111]$; λ(detection)$=638$ nm; $T=1.4$ K; amplitude modulation of magnetic field is 2.0 G (peak to peak) in (a), (b), and (c), and 0.2 G (peak to peak) in (d). Phase-sensitive detection is at 30 Hz. (a) Field scan 0–400 G, (b) field scan 450–650 G, (c) field scan 900–1200 G, (d) field scan 485–545 G.

burning experiments.[6] More specifically, sudden reductions have been observed in the depth of an optical hole, burned in the 638-nm absorption line, for the above-given magnetic field strengths. The optical hole-burning studies showed the following. (i) When $H=514$ G, cross relaxation involving N-V centers with principal axes along the magnetic field direction and P_1 centers takes place. [A P_1 center consists of a substitutional nitrogen atom and has a net spin of $S=\frac{1}{2}$ (Ref. 13).] (ii) When $H=600$ G, cross relaxation arises because the subset of N-V centers with their main axes parallel to H becomes resonant with all other (orientationally inequivalent) N-V centers; the latter have their main molecular axes at an angle of 109°28′ with respect to H. (iii) When the field is rotated away from the [111] direction, the magnetic field can be tuned in such a way that the triplet sublevels of a specific N-V site are equally spaced. Under these circumstances, two (out of the three) spin transitions within the triplet become resonant and an enhanced cross relaxation between magnetically equivalent N-V centers is found. This case will be referred to as autocrossing. (iv) When $H=1030$ G ($\mathbf{H}\|[111]$), level-anticrossing phenomena occur for those centers with their main axes along H.

The signals of Fig. 2 show that cross-relaxation and level-anticrossing situations also give rise to abrupt changes in the N-V center *emission* intensity. Furthermore, the angular dependence of these signals was found to follow the anisotropic pattern previously reported for the hole-burned signal in optical absorption.[6] The hyperfine splittings of $A_{\|}=39$ G and $A_{\perp}=29$ G as observed for the resonance at $H=514$ G in Fig. 2(d) is characteristic of hyperfine interactions with the $I=1$ spin of the nitrogen nucleus in the P_1 center.[13]

B. Optically detected stimulated spin-echo transients

Time-resolved spin coherence experiments were performed to study the spin dynamics of the CR and LAC processes. The applicability of techniques for the optical detection of spin-coherent transients in zero field for the diamond N-V center system has been established previously.[5] Here the measurements have been extended in the presence of magnetic fields along [111] and [001] directions. First of all, optically detected Hahn echo decay transients were measured in magnetic fields up to about 1000 G. Unexpectedly, upon the application of small fields (up to 200 G) strong nuclear modulation effects were observed in the decay transients. No such modulations were found in the Hahn echo decay in zero field. Analysis of the results showed that upon the application of a small field, hyperfine interactions due to the 1% abundant ^{13}C ($I=\frac{1}{2}$) spins in the lattice are picked up by the N-V center triplet spins. A full discussion of these effects is outside the scope of this paper, however, and will be presented in a forthcoming paper elsewhere.[14]

Upon the application of a magnetic field, also the decay kinetics of the Hahn echo amplitude is influenced. For example, we find that the Hahn echo decays with a characteristic decay time of about 80 μs when the magnetic field has a value such that CR among the N-V centers is absent. In zero field and when $H=600$ G, however, the decay time is reduced to 40 μs. Obviously, CR appreciably affects the Hahn echo decay rate. As shown elsewhere,[14] the Hahn echo decay kinetics is not fully determined by the spin-spin interactions within the N-V centers alone, but, to a large extent, depends also on the hyperfine interactions within the N-V center. This is not the case for stimulated spin-echo and spin-locking decay transients and this is the main reason why in the remainder of this paper we focus on the SED and SLD results only.

In the optically detected stimulated spin-echo decay experiments, a $\pi/2$-τ-$\pi/2$-T-$\pi/2$-τ-$\pi/2$ pulse sequence is applied, where the final $\pi/2$ pulse is meant to optically probe the residual stimulated echo at $2\tau+T$, as T is increased.[7] Figure 3 shows the observed stimulated-echo decay in zero field and for fields of 150 G, along [111] and [001] directions, respectively. Clearly, the stimulated-echo amplitude decay slows down when a small magnetic field is applied along the [111] direction; for $\mathbf{H}$ along [001], no significant change in the stimulated-echo decay rate is observed. These results illustrate the influence of cross relaxation on the echo decay: in zero field and for $\mathbf{H}$ along a [001] crystallographic axis, i.e., when all N-V center sites are magnetically equivalent, CR among these sites contributes to the rate at which the steady state population upon cw optical excitation is achieved. In a field along the [111] direction, however, (H not equal to 600 G) the majority of N-V centers (namely those with molec-

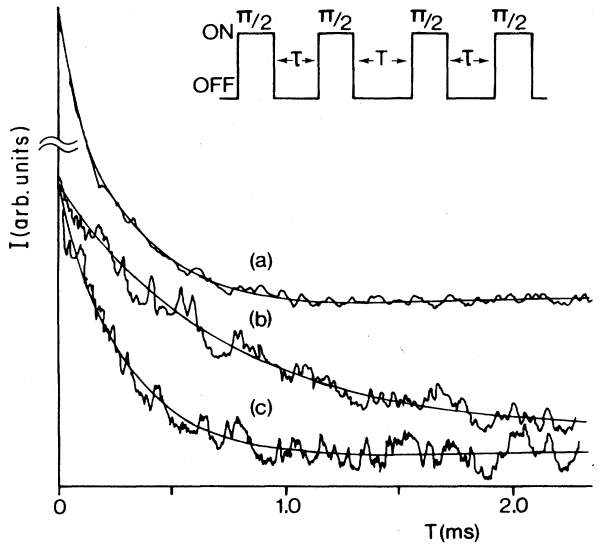

FIG. 3. Optically detected stimulated-echo decay curves for the N-V center ($T=1.4$ K) (a) in zero field, (b) $H=150$ G, $\mathbf{H}\|[111]$, as probed for N-V defects of subensemble I, (c) $H=150$ G, $\mathbf{H}\|[001]$. Drawn curves represent monoexponential fits with (a) $T_d=250$ μs, (b) $T_d=810$ μs, (c) $T_d=250$ μs. Inset shows applied microwave pulse sequence for optical detection of stimulated-echo decay signals. In (a), (b), and (c), $\tau=3.0$ μs.

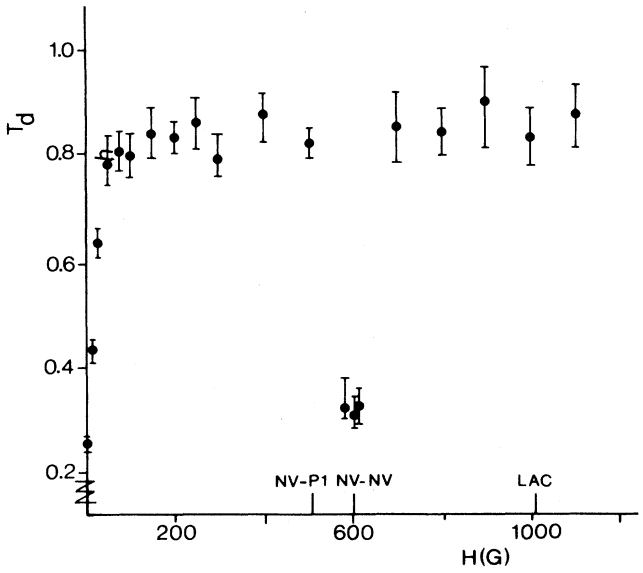

FIG. 4. Magnetic field dependence of the characteristic stimulated-echo decay time T_d (ms), representative of the N-V centers of subensemble I ($\mathbf{H}\|[111]$). The time interval τ in all stimulated-echo experiments was given the constant value of 3.0 μs. The magnetic field values for which CR and LAC occur are also indicated.

ular main axes at an angle of 109°28′ to H) is no longer resonant with the N-V centers with main axes along H and for which the spin transition is pumped in the echo experiment. Thus in general the magnetic field lifts the conditions for cross relaxation and the relaxation of the stimulated-echo amplitude slows down.

Figure 4 shows the characteristic decay times T_d, as determined by fitting the experimental stimulated-echo decays, as obtained for a number of different magnetic fields along [111], to monoexponentially decaying functions. The results show that the stimulated-echo decay rate is fairly constant with a decay time of about 820 μs, except when CR occurs. For $H=0$ and $H=600$ G, all N-V sites are involved in CR and we obtain $T_d=250$ and 300 μs, respectively. Hence, an enhancement of the stimulated-echo decay rate is observed when CR takes place.

When the magnetic field direction is turned away from the [111] direction, the phenomenon of autocrossing involving resonant α-β and β-γ transitions of magnetically equivalent centers may be observed. Autocrossing is manifested as a sudden change of the 638-nm emission intensity when certain magnetic field strengths are applied. E. g., if $\mathbf{H}$ is rotated by an angle of 25° from the [111] direction, the emission intensity changes are observed when H equals 450 G. For the same crystal orientation, we have also measured the stimulated-echo decay transients for a number of different magnetic field strengths. A constant value of 820 μs for the characteristic SED time is found regardless of the field strength, except when $H=450$ G, then we find approximately 350 μs. Thus, as for the CR conditions when $\mathbf{H}\|[111]$, an enhancement of the SED rate constant is found although the enhancement factor is a little less than the factor 3 in the case of CR between magnetically inequivalent sites. Finally, for applied magnetic fields for which N-V centers show cross relaxation with P_1 centers (e.g., for a field of 514 G along the [111] direction), no enhancement of the stimulated-echo decay is observed (cf. Fig. 4.).

C. Optically detected spin-locking transients

The influence of CR has also been verified in decay transients of the N-V center in the spin-locked state. In this experiment, the applied microwave pulse sequence for the triplet-spin transition is $\pi/2$-90°-τ_1-90°-$\pi/2$.[15] Controlled switching of the phase of the microwave field over 90° immediately after the spin coherence preparation pulse, aligns the rotating spin polarization parallel to the microwave H_1 component. Relaxation due to perturbing interactions for the N-V centers larger than the strength of the locking microwave H_1 field is probed when τ_1 is increased. A few characteristic spin-locking echo decay results, for $H=0$ and $H=150$ G (along [111] and [001] directions, respectively), are displayed in Fig. 5. The figure includes the fittings to monoexponentially decaying functions. The results show that the spin-locking decay time ($T_{1\rho}$) at zero field and for $\mathbf{H}\|[001]$ is given as $T_{1\rho}\sim 2.0$ ms, whereas for $\mathbf{H}\|[111]$ the spin-locking decay time is $T_{1\rho}=4.0$ ms. The experimental results for the spin-locking relaxation rate constant as a function of externally applied fields along [111] are displayed in Fig.

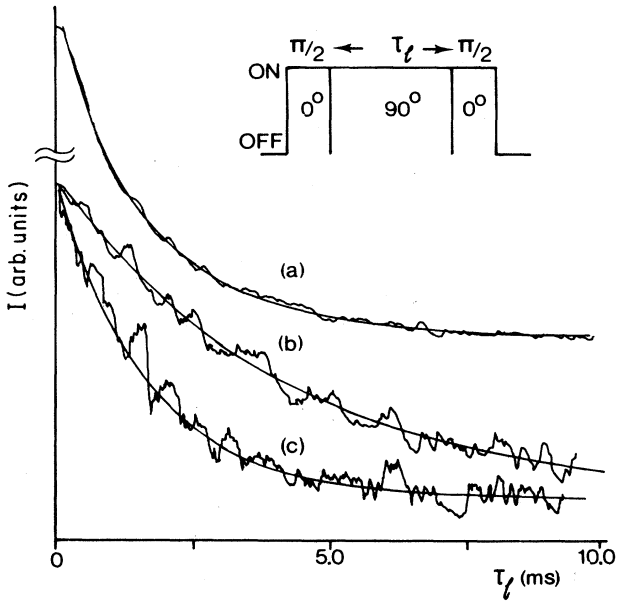

FIG. 5. Optically detected spin-locking echo decay curves for the N-V center ($T=1.4$ K) (a) in zero field, (b) $H=150$ G, $\mathbf{H}\|[111]$ as probed for N-V defects of subensemble I, (c) $H=150$ G, $\mathbf{H}\|[001]$. Drawn curves represent monoexponential fits with (a) $T_{1\rho}=1.9$ ms, (b) $T_{1\rho}=4.2$ ms, (c) $T_{1\rho}=2.0$ ms. In (a), (b), and (c) the laser power used for optical excitation at 514 nm was maintained at 200 mW. Inset shows applied microwave pulse sequence for optical detection of spin-locking decay echo signals.

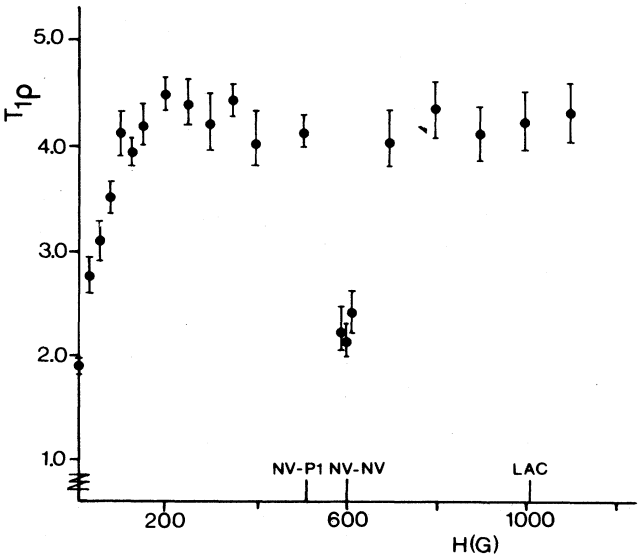

FIG. 6. Magnetic field dependence of the characteristic spin-locking echo decay time $T_{1\rho}$ (ms), representative of the N-V centers belonging to subensemble I ($\mathbf{H}\|[111]$). The laser power used for optical excitation at 514 nm was maintained at 200 mW. The magnetic field values for which CR and LAC occur are as indicated.

6. The spin-locking decay rate is, like the decay rate of the stimulated spin echo, almost independent of the applied field ($T_{1\rho}\sim 4.1$ ms) except when H is near zero field, or 600 G, i.e., when CR involving different N-V center sites is possible. In the latter situation, $T_{1\rho}\sim 2.0$ ms. When $H=514$ or 1030 G, i.e., when N-V centers show CR with P_1 centers and LAC effects, respectively, we still find $T_{1\rho}\sim 4.1$ ms. Under autocrossing conditions ($H=450$ G, H is almost along the [110] direction), the measured spin-locking time is found as $T_{1\rho}\sim 2.5$ ms.

V. DISCUSSION

As already remarked in Sec. IV A, the observed resonances of Fig. 2 in the emission intensity of the N-V center diamond system are analogous to those previously reported for optical hole burning in absorption.[6] Evidently, CR and LAC affects the population distribution of the optically probed spin sublevels in the triplet ground state and since photoexcitation is a spin-selective process, the population of the fluorescent excited state is also affected by CR and LAC. As discussed previously,[6] CR arises here because of energy-conserving spin flip-flops between the subgroup of centers that is spin-polarized by optical excitation and the vast majority of nonexcited triplet centers. The latter centers not only comprise equivalently oriented centers, but for certain magnetic field strengths and orientations, there is in addition accidental resonance with magnetically nonequivalent centers. The result of the flip-flop communication between subensembles I and II is additional and thus faster relaxation. As will be reported elsewhere,[14] in a magnetic field subensembles I and II exhibit in optical absorption a difference in extinction, and therefore when under CR conditions part of the spin alignment in subensemble I leaks away into subensemble II, a change in the population of the triplet-spin levels of the optically probed defects belonging to subensemble I will result. The latter phenomenon in fact is reflected by the abrupt emission intensity changes shown in Fig. 2.

The stimulated-echo decay constants show an enhancement of the SED rate constant by a little more than a factor 3, when a magnetic field is applied such that CR conditions prevail (see also Fig. 4). This result is in good agreement with the predictions discussed in Sec. II. The stimulated-echo decay of the N-V center system is therefore associated with a spin diffusion process arising from (dynamical) magnetic dipole-dipole interactions among the N-V centers themselves.

The results of the spin-locking decay experiments are analogous. As is well known,[16] the spin-locked signal decays due to time-dependent perturbations experienced by the probed spins, the perturbation being larger than the coupling of the locked spins to the microwave H_1 field. Since in the spin-locking experiment only the larger jumps in frequency space due to the dynamical spin-spin interactions between A and B spins are probed, it will be evident that the spin-locking decay rate will be much slower (in our experiments by almost an order of magnitude) than the decay of the stimulated spin echo which includes contributions of all possible frequency steps in

the spin diffusion process. Population changes induced by spin-lattice relaxation or depletion of the ground-state population by photoexcitation of the probed N-V centers will also contribute to the spin-locking signal decay.

To obtain the contribution of spin-spin-induced diffusion to the spin-locking decay, the observed decay rate must be corrected for the contribution of the population relaxation process. The population relaxation decay was separately determined by means of an adiabatic rapid passage experiment. The lifetimes of the individual spin sublevels, at 1.4 K and in zero field, were found to be 4.5 and 23.9 ms, respectively, when using for optical excitation of the N-V center a laser power of 200 mW. The lifetimes were found to be completely determined by the intensity of the laser power applied in the optical pumping cycle. Thus in the spin-locked state, population depletion due to the optical excitation occurs at a rate of $\frac{1}{2}(2.2\times10^2+4.2\times10^1)\ s^{-1}=1.3\times10^2\ s^{-1}$. Experimentally, in zero field the spin-locking signal is found to decay at a rate of $(5.3\pm0.2)\times10^2\ s^{-1}$, so the contribution of the spin diffusion to the spin-locking decay rate is found to be $4.0\times10^2\ s^{-1}$.

The contribution of spin diffusion to the spin-locking decay rate constant has recently also been obtained independently in a different way.[5] From a study of the influence of the intensity of the exciting light on the spin-locking decay rate it was shown that the spin-lock decay slows down as the power of the exciting light was decreased. Extrapolation to zero excitation intensity yielded a residual spin-locking decay rate of $3.9\times10^2\ s^{-1}$. This value has to be compared with the rate of $4.0\times10^2\ s^{-1}$ mentioned above as obtained after correcting the measured spin-locking decay constant for the laser-induced population depletion. We thus take the spin-diffusion-induced decay as $4.0\times10^2\ s^{-1}$. In the same manner, the spin-locking decay constant corrected for population depletion was obtained for the system in a magnetic field of 200 G; the result is $(1.2\pm0.2)\times10^2\ s^{-1}$. The experimental data thus imply that the spin-locking decay rate constant is reduced by a factor of a little more than 3 when a magnetic field is applied in such a way that magnetically inequivalent subensembles (of type I and II) exist. This result is compatible with the calculated change for $\bar{K}_1$ when CR conditions are lifted by the application of a magnetic field (cf. Table I). Again we conclude, as from the SED results, that the major part of the CR dynamics in zero field is accounted for by magnetic dipole-dipole interactions between the N-V centers themselves.

The case of autocrossing has not been treated explicitly in Sec. II. Autocrossing also contributes to an enhanced spin relaxation because the autocorrelation functions $\langle d_{xB}d_{xB}(t_c)\rangle$ and $\langle d_{yB}d_{yB}(t_c)\rangle$ in Eqs. (9) and (10) then contain oscillatory factors at a frequency of $\omega_{\alpha\beta}$ and the magnetic field is such that $\omega^B_{\alpha\beta}=\omega^A_{\beta\gamma}$. Of course, the relative change for the SED rate will be less than for the above-treated cases of CR because only magnetically equivalent N-V centers belonging to subensemble I can participate in the autocrossing process.

Finally, it is briefly discussed that no changes in the coherent transients of the N-V center triplet spin system are found when, in a magnetic field, CR between the N-V centers and resonant P_1 centers occurs. The result is readily explained by a consideration of the very small line width of the $S=\frac{1}{2}$ spin transition of the P_1 center. EPR measurements of the P_1-center spin transition, when $H\simeq3300$ G, revealed an inhomogeneous line width (full width at half maximum) of about 100 kHz. On the other hand, in measurements of coherent transients (e.g., stimulated spin echo decay), the ensemble of spins for which the coherence is probed have microwave resonance frequencies with an inhomogeneous spread of at least 3 MHz (i.e., the Rabi frequency in our experiments). In the coherent experiments therefore, the cross relaxation with P_1 centers affects only a small fraction of the excited triplet spins and its effect on the overall spin coherence decay may be ignored.

VI. CONCLUSION

A major result of the experimental study presented in this paper is that spin diffusion in the ensemble of N-V centers, in the triplet ground state, occurs due to intercenter magnetic dipole-dipole interactions on a time scale ranging from a few hundred microseconds up to milliseconds. In addition, at the low temperatures of the experiments ($T\simeq1.4$ K), for the N-V centers in diamond the spin-lattice relaxation is almost frozen out (T_1 is larger than 1 s). Upon optical excitation of the N-V centers, an appreciable spin alignment is set up in the ensemble. The spin alignment is favored by the strong thermal isolation of the triplet spins from the lattice modes. Moreover, although the magnetic dipole-dipole interactions facilitate a rapid establishment of a common spin temperature in the bath of triplet spins, the flip-flop processes cannot alleviate the spin alignment. Thus, eventually in steady state, the magnitude of the optically induced spin alignment is solely determined by the balance of the kinetics involved in the optical pumping and the spin-lattice relaxation processes.

ACKNOWLEDGMENTS

The authors thank Keith Holliday and Neil Manson (Laser Physics Centre, Australian National University, Canberra) for discussions. One of us (M.G.) acknowledges the John van Geuns Fonds for additional support. In part this work has been supported by the Netherlands Foundation for Chemical Research (SON) with financial aid from the Netherlands Organization for Scientific Research (NWO).

[1] G. Davies and M. F. Hamer, Proc. R. Soc. London, Ser. A **348**, 285 (1976).

[2] J. H. N. Loubser and J. H. van Wyk, Diamond Res. **11**, 4 (1977); Rep. Prog. Phys. **41**, 1202 (1978).

[3] P. D. Bloch, W. S. Brocklesby, R. T. Harley, and M. J. Henderson, J. Phys. (Paris) Colloq. **C7**, 527 (1985).

[4] N. R. S. Reddy, N. B. Manson, and E. R. Krausz, J. Lumin. **38**, 46 (1987).

[5]E. van Oort, N. B. Manson, and M. Glasbeek, J. Phys. C **21**, 4385 (1988).
[6]K. Holliday, N. B. Manson, M. Glasbeek, and E. van Oort, J. Phys. Cond. Matter (to be published).
[7]W. G. Breiland, H. C. Brenner, and C. B. Harris J. Chem. Phys. **62**, 3458 (1975); H. C. Brenner, in *Triplet State ODMR Spectroscopy,* edited by R. H. Clarke (Wiley, New York, 1982), p. 185.
[8]M. Glasbeek and R. Hond, Phys. Rev. B **23**, 4220 (1981).
[9]R. Hond and M. Glasbeek, Phys. Rev. B **26**, 427 (1982).
[10]R. W. Zwanzig, in *Lectures in Theoretical Physics,* edited by W. E. Britten, B. W. Downs, and J. Downs (Interscience, New York, 1961), Vol. **3**, p. 106; H. Mori, Prog. Theor. Phys. **33**, 423 (1965).
[11]B. J. Berne, in *Statistical Mechanics, Part B: Time-Dependent Processes,* edited by B. J. Berne (Plenum, New York, 1977), p. 233.
[12]M. Glasbeek and R. Vreeker, Chem. Phys. **89**, 111 (1984).
[13]W. V. Smith, P. P. Sorokin, I. L. Gelles, and G. J. Lasher, Phys. Rev. **115**, 1546 (1959).
[14]E. van Oort and M. Glasbeek (unpublished).
[15]R. Vreeker, M. Glasbeek, E. T. Sleva, and A. H. Zewail, Chem. Phys. Lett. **129**, 11 (1986).
[16]C. P. Slichter, *Principles of Magnetic Resonance* (Springer, Berlin, 1978).